Advanced Materials Research
ISSN: 1662-8985, Vols. 989-994, pp 548-551
doi:10.4028/www.scientific.net/AMR.989-994.548

Submitted: 2014-05-25
Accepted: 2014-05-30
Online: 2014-07-16

The Finite Element Simulation of Thermal Deformation and Microstructure Evolution Forecast of AZ61 Alloy

Quan Li[1,a], Wenjun Liu[1,2], Renju Cheng[1], Cheng Li[1],Shan Jiang[1], Suqin Luo[1],Xianquan Jiang[1], Fusheng Pan[1,2]

[1]Chongqing Academy of Science and Technology, Chongqing 401123, China
[2]College of Materials Science & Engineering, Chongqing University, Chongqing 400030, China

[a]156723583@qq.com

Keywords: Magnesium alloy, Finite element, Simulation, Forecast

Abstract: In this paper, rigid-plastic finite element simulation software Marc / Auto-forge reflect compression AZ61B magnesium alloy case. Simulation results show that the stress, strain and temperature distribution within the sample is uneven, uneven distribution affect the organization, and with the changes in the deformation process and calculation results with the experimental data exactly. The finite element method can be used in the actual production forecast after tissue deformation components, optimization of process parameters to control the quality of the finished piece.

1 Introduction

Metal temperature of various parts of the work piece and tooling, different stress during hot deformation, and microstructural evolution during deformation is closely associated with these factors. Based on the basic theory of rigid-plastic finite element, finite element simulation software Marc / Auto-forge, AZ61 magnesium alloy thermal compression process further simulation and analysis, analysis of thermal deformation of AZ61 magnesium alloy, and the evolution of the microstructure results were forecasts.

2 Sample finite element model

Cylindrical sample is Φ15 × 20mm, and to reduce the computation time, the symmetry of the sample, take half as analog objects. Take a four-node quadrilateral element model of division 48 units and 65 nodes. Analysis method using an updated Lagrange method described thermal coupling large deformation rigid-plastic finite element method, the use of the material yield criterion Von Mises criterion.

Boundary conditions:

(1) boundary conditions: all nodes cylindrical symmetry axis of the sample in the x-direction displacement is zero, ux = 0.

(2) friction conditions: between deformation tools and rolling contact surfaces follow Coulomb friction coefficient between the die and the sample taken 0.2.

(3) heat transfer boundary conditions[1]: the presence of the free surface of the sample and the cycle of convective and radiative heat transfer environment. There is no contact between the sample heat when in contact with the mold. The first two boundary conditions referred to in the third boundary condition in heat transfer. Can be written as a unified formula:

$$q = -\lambda\left[\frac{\partial t}{\partial n}\right] = \alpha\left(t - t_{\infty}\right)$$

In the formula, t is the surface temperature, t_{∞} is the ambient temperature, α is the heat transfer coefficient.

Convective heat transfer coefficient environment take 0.17KW/m2 • K according to test conditions. And radiation heat transfer coefficient between the environment in accordance with the laws of the radiation is converted into other small radiation heat transfer coefficient can be expressed by the following formula based on radiation law[2-3].

$$h_r = \sigma\varepsilon\left(t + t_\infty\right)\left(t^2 + t_\infty{}^2\right)$$

In the formula, σ is the Boltzmann constant, σ = 5.67 × 10-11KW/m2K4, ε thermal emissivity material, 0.15[4].

Thermal contact between the sample and mold simplified contact heat conduction problems with the contact between the two solid thermal conductivity, paper = 20 KW/m2 • K. Ambient temperature and mold temperature, and were taken 20 ℃ 350 ℃. The thermal deformation of metal deformation, thermal power conversion factor of 0.9. Further, the sample contacting surface and the mold will produce frictional heat, the heat is distributed evenly to the parts of the specimen and the mold[5-6].

3 Simulation results and analysis

3.1 Equivalent strain distribution

Figure 1 is a sample of AZ61 magnesium alloy at different deformation temperature equivalent strain distribution. Be seen, the equivalent strain of the sample is very uneven in the top of the sample, due to friction, the minimum strain, and the sample portion and the corner portion of a sample core greatly deformed. Other parts of the deformation distribution be between the maximum and minimum by the Ministry to the top of the heart, the center to the edge showed a decreasing trend. Can also be seen from Figure 1, as the temperature increases, the deformation easily throughout the strain increases at a lower temperature (300 ℃ to 400 ℃) increase in the amount of more instructions corresponding to the temperature variables influenced; but at around 450 ℃, 400 ℃ to reduce the amount of increase, indicating less affected by temperature corresponding variables.

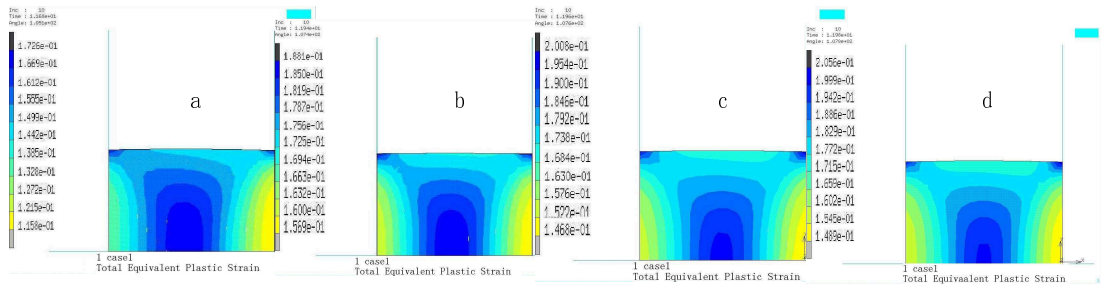

Fig.1 Equivalent strain distribution during the deformation step 10
(a: deformation temperature 300 ℃, strain rate of 0.01s^{-1}; b: deformation temperature 350 ℃, strain rate of 0.01s^{-1}; c: deformation temperature 400 ℃, strain rate 0.01s^{-1}; d: deformation temperature 450 ℃, strain rate 0.01s^{-1})

3.2 Equivalent stress distribution

Figure 2 is the effective stress variation with temperature distribution seen from the figure, the force effect of the sample and a very uniform, the top of the sample, due to friction, the minimum strain, and the sample and the sample angle core section deformed great. Other parts of the distribution between the maximum and minimum distortion between the central portion by the top edge portion to the central portion showed a decreasing trend with increasing temperature, easily deformed, the entire stress increases, but the increase in the amount of not more than , indicating little effect of temperature on the strain.

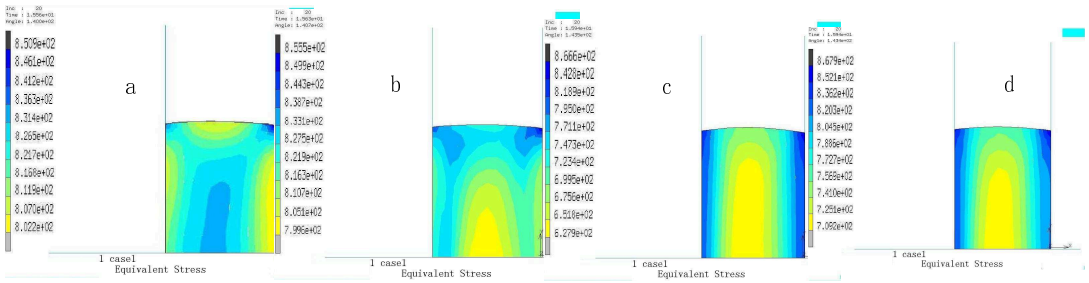

Fig.2 Mises stress distribution of deformation at Step 20

(a: deformation temperature 300 ℃, strain rate of 0.01s^{-1}; b: deformation temperature 350 ℃, strain rate of 0.01s^{-1}; c: deformation temperature 400 ℃, strain rate 0.01s^{-1}; d: deformation temperature 450 ℃, strain rate 0.01s^{-1})

3.3 Temperature distribution

Figure 3 shows the temperature distribution at different strain rates throughout the sample. Since the thermal conductivity of the sample surface exists between the presence of convection and radiation heat, top of the sample and mold, so the temperature decreases from the inside and outside. At low strain rate, prolonged heat and thermal conductivity, high temperature deformation rate when compared to low. Further, the deformation rate increases, an increase in the plastic work, the conversion of heat also increased, thereby increasing the temperature of the sample. Deformation rate of 0.01s-1, the internal temperature of the sample is less than the deformation temperature, when the strain rate 0.1s-1, the temperature of the sample over the central portion deformation temperature. In another modification of the same condition, the amount of deformation increases, the time required to deform at low extension, thus lower the sample temperature.

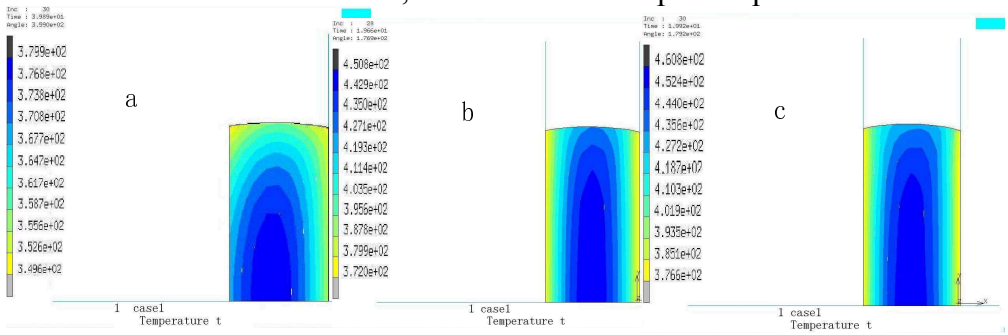

Fig.3 Deformation temperature distribution at step 30

(a: deformation temperature 350 ℃, strain rate of 0.01s^{-1}; b: deformation temperature 350 ℃, strain rate of 0.1s^{-1}; c: deformation temperature 350 ℃, strain rate 1s^{-1})

3.4 Tissue distribution of dynamic recrystallization

Figure 4 is a dynamic recrystallization grain size distribution, in each case, the uneven distribution of the grain sample. Heart large specimen deformed grains relatively small; while reducing the amount of deformation from the inside out, recrystallized grain size also increases. Deformation temperature, the grain size becomes large accordingly, and the strain rate increases, the grain size becomes smaller.

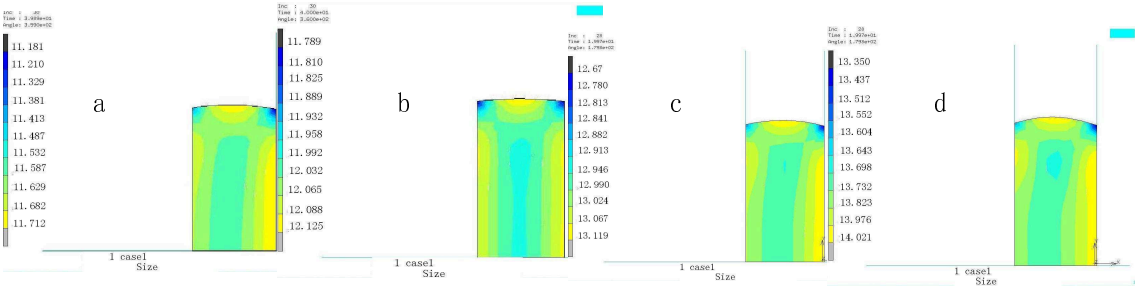

Fig.4 Grain size distribution at Step 20

(a: deformation temperature 300 ℃, strain rate of 0.01s^{-1}; b: deformation temperature 350 ℃, strain rate of 0.01s^{-1}; c: deformation temperature 400 ℃, strain rate 0.01s^{-1}; d: deformation temperature 450 ℃, strain rate 0.01s^{-1})

4 Conclusions

In this paper, the rigid-plastic finite element simulation software Marc / Auto-forge consider the coupling of heat transfer and deformation, and can reflect more fully the compression deformation of AZ61B magnesium alloy. Simulation results show that the stress, strain, temperature inside the uneven distribution of the sample, with a corresponding impact on tissue distribution is not uniform and varies with the deformation process, comparing the calculation results with the experimental data prove the finite element method used herein have higher accuracy in reference to the actual production can predict the deformation member, optimize the process parameters to control the quality of the finished piece.

Acknowledgement

This work is supported by the Chongqing High-level Overseas Talent Base Construction Projects; International Science and Technology Cooperation Project (2013DFA71070); Chongqing International Science and Technology Cooperation Base Project (cstc2011gjhz50001)

References

[1] S.F.Wong, P.D.Hodgson, C.J.Chong, P.F.Thomson. Physical Modeling with Application to Metal Working, especially to Hot Rolling. J.Mater.Process.technol.1996,62:260－274.

[2] P.R.Ding, D.Y.Ju, S.Imatani, T.Inoue. Numerical Simulation of Coupled Thermo－Mechanical Behavior of a Cylinder Billet During Hot-forging Process. Journal of Shanghai Jiaotong University. 2000, 5(1):263－269.

[3] NIU JI-tai, SUM LEI-Jian, LI HAI-tao. research micro-alloy hot-rolled austenitic grain size model based on artificial neural networks, Materials Science and Technology, 1997,7 (1) 12-16.

[4] XIA SHAN-mu, Li DA-yong. the mechanical properties of cast iron for fast prediction of artificial neural networks, Applied Sciences, 2002,20 (3) :309-312.

[5] DAI QI-Xun, DAI XI-Min. Journal of Neural Network in austenitic steel design Steel Research, 1997,9 (6) :37-40.

[6] LIU XUE-feng, WANG LING-yun, artificial neural network model aluminum-lithium alloy high temperature deformation flow stress of Chongqing University (Natural Science Edition), 2001,24 (2).